

ON THE HETEROGENEITY OF METAL-LINE AND Ly α ABSORPTION IN GALAXY “HALOS” AT $z \sim 0.7$

CHRISTOPHER W. CHURCHILL¹, GLENN G. KACPRZAK¹,
 CHARLES C. STEIDEL², AND JESSICA L. EVANS¹

Accepted: *Astrophysical Journal* (12/06)

ABSTRACT

We examine the properties of two galaxy “halos” at $z \sim 0.7$ in the TON 153 ($z_{\text{em}} = 1.01$) quasar field. The first absorber–galaxy pair (G1) is a $z = 0.672$, $L_B = 4.3 L_B^*$, E/S0 galaxy probed at $D = 58$ kpc. G1 is associated with a remarkable five–component Ly α complex having $\tau_{\text{LL}} \leq 0.4$, $W_r(\text{Ly}\alpha) = 2.8 \text{ \AA}$, and a velocity spread of $\Delta v = 1420 \text{ km s}^{-1}$. We find no Mg II, C IV, N V, nor O VI absorption in these clouds and infer metallicity upper limits of $-3 \leq \log Z/Z_\odot \leq -1$, depending upon assumptions of photoionized or collisionally ionized gas. The second absorber–galaxy pair (G2) is a $z = 0.661$, $L_B = 1.8 L_B^*$, Sab galaxy probed at $D = 103$ kpc. G2 is associated with metal–enriched ($\log Z/Z_\odot \simeq -0.4$) photoionized gas having $N(\text{H I}) \simeq 18.3 \text{ [cm}^{-2}\text{]}$ and a velocity spread of $\Delta v = 200 \text{ km s}^{-1}$. The very different G1 and G2 systems both have gas–galaxy properties inconsistent with the standard luminosity dependent galaxy “halo” model commonly invoked for quasar absorption line surveys. We emphasize that mounting evidence is revealing that extended galactic gaseous envelopes in the regime of $D \leq 100$ kpc do not exhibit a level of homogeneity supporting a standardized halo model. Selection effects may have played a central role in the development of a simple model. We discuss the G1 and G2 systems in the context of Λ CDM models of galaxy formation and suggest that the heterogeneous properties of absorber–galaxy pairs is likely related to the range of overdensities from which galaxies and gas structures arise.

Subject headings: galaxies: halos, evolution — quasars: individual (TON 153)

1. INTRODUCTION

Observations of baryonic gas in galaxy halos constrain galaxy evolution models, in particular the successful Λ CDM model of structure formation. However, important quandaries persist, including the overcooling (e.g., White & Rees 1978) and baryon fraction problems (e.g., Mo & Mao 2002), in which the cooling of baryonic gas is too efficient, resulting in compact halos and highly peaked rotation curves inconsistent with the Tully–Fisher relationship (Mo et al. 1998). Samples of galaxy–absorber pairs in quasar absorption line surveys of Ly α $\lambda 1215$ (Lanzetta et al. 1995; Chen et al. 1998, 2001b), Mg II $\lambda \lambda 2796, 2803$ (Bergeron & Boissé 1991; Le Brun et al. 1993; Steidel, Dickinson, & Persson 1994; Steidel et al. 1997; Churchill, Kacprzak, & Steidel 2005), C IV $\lambda \lambda 1548, 1550$ (Chen et al. 2001a), and O VI $\lambda \lambda 1031, 1037$ (Sembach et al. 2004; Tripp & Bowen 2005; Tumlinson et al. 2005; Tripp et al. 2006) absorption provide key data for addressing the overarching question—what processes regulate and sustain the baryon fraction and kinematic, chemical and ionization conditions of galaxy halos in the context of Λ CDM models?

The gas boundaries of “absorption selected” galaxies are characterized using the Holmberg–like (Holmberg 1975) relationship,

$$R(L) = R^* \left(\frac{L_B}{L_B^*} \right)^\beta, \quad (1)$$

where R^* is the halo size for an L^* galaxy, which scales as $R^* \propto [(dN/dz)/(C_f f_{\text{gal}} \mathcal{K})]^{1/2}$, where dN/dz is the absorption redshift path density, C_f is the covering factor, f_{gal} is the fraction of galaxies with absorbing halos, and \mathcal{K} is the geometry factor ($\mathcal{K} = 0.5$ for thin disks; $\mathcal{K} = 1$ for spherical). Estimates

of R^* and β apply to surveys conducted to a fixed absorption sensitivity for a given ion/transition and employ the galaxy luminosity function (see Lanzetta et al. 1995).

For Mg II absorbers with $W_r(2796) \geq 0.3 \text{ \AA}$, Steidel (1995) reported $R^* = 55 \text{ kpc}^3$, $\beta = 0.2$, and $C_f f_{\text{gal}} \mathcal{K} = 1$. Lyman limit systems (LLS, $\tau_{\text{LL}} \geq 1$) show one–to–one correspondence with $W_r(2796) \geq 0.3 \text{ \AA}$ Mg II absorption (Churchill et al. 2000a) and have virtually identical dN/dz (Stengler–Larrea et al. 1995). Statistically, LLS have $R^* \simeq 55 \text{ kpc}$ for an *assumed* $C_f f_{\text{gal}} \mathcal{K} = 1$. For Ly α absorption with $W_r(\text{Ly}\alpha) \geq 0.30 \text{ \AA}$, Chen et al. (1998, 2001b) reported $C_f f_{\text{gal}} \mathcal{K} = 1$ within $R^* = 310 \text{ kpc}$ with $\beta = 0.39$. For C IV systems with $W_r(1548) \geq 0.17 \text{ \AA}$, Chen et al. (2001a) found $R^* = 170 \text{ kpc}$ and $\beta = 0.5$, and deduce $C_f f_{\text{gal}} \mathcal{K} = 1$. There are few constraints for O VI absorption, which may commonly arise in the warm–hot intergalactic medium (Davé et al. 1998, 2001, however, see Tumlinson et al. 2005; Tripp et al. 2006).

A possible source of bias toward deducing $C_f f_{\text{gal}} \mathcal{K} = 1$, is that the presence of a gas “halo” is requisite for the inclusion of an absorber–galaxy pair in an absorption selected sample. Establishing the absorption *ex post facto* galaxy identifications has yielded $C_f f_{\text{gal}} \mathcal{K} < 1$; Bechtold & Ellingson (1992) reported $C_f f_{\text{gal}} \mathcal{K} \simeq 0.25$ for $W_r(2796) \geq 0.26 \text{ \AA}$ (3σ) with $D \leq 85 \text{ kpc}$ and Tripp & Bowen (2005) reported $C_f f_{\text{gal}} \mathcal{K} \sim 0.5$ for $W_r(2796) \geq 0.15 \text{ \AA}$ (3σ) with $D \leq 50 \text{ kpc}$. For $W_r(2796) \geq 0.02 \text{ \AA}$ (5σ), Churchill, Kacprzak, & Steidel (2005) reported that very weak Mg II absorption arises both well *inside and outside* the $R(L)$ boundary of bright galaxies. Churchill et al. also find $W_r(2796) > 1 \text{ \AA}$ absorption out to $\simeq 2R(L)$ in several cases. Since $\tau_{\text{LL}} < 1$ H I traces weak Mg II and $\tau_{\text{LL}} > 1$ H I traces strong Mg II (Churchill et al. 2000a),

³ Throughout this paper, we adopt a $H_0 = 70 \text{ km s}^{-1} \text{ Mpc}^{-1}$, $\Omega_m = 0.3$, and $\Omega_\Lambda = 0.7$ cosmology. We have converted all cosmology dependent physical quantities taken from the literature to this cosmology, unless explicitly stated.

¹ New Mexico State University, Las Cruces, NM 88003 cwc, glennk, jlevans@nmsu.edu

² Caltech, Pasadena, CA 91125 ccs@astro.caltech.edu

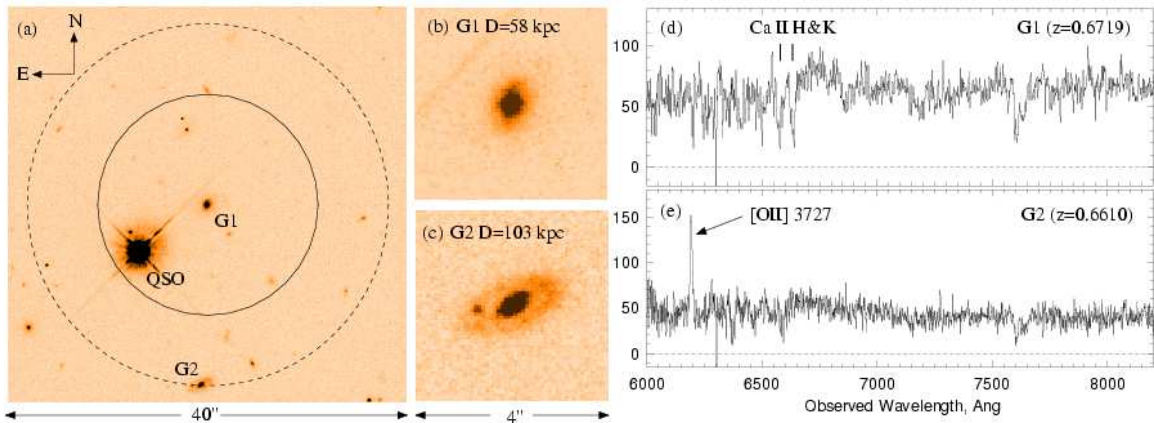


FIG. 1.— (a) A $40'' \times 40''$ section of the F702W WFPC-2 image of the TON 153 field centered on galaxy G1. The solid circle represents a $R(L) = 73$ kpc halo for $W_r(2796) \geq 0.3 \text{ \AA}$ and for LLS absorption. The dashed circle represents a $R(L) = 123$ kpc halo for $W_r(2796) \geq 0.02 \text{ \AA}$. — (b,c) $4'' \times 4''$ images of G1 and G2. — (d,e) The Keck/LRIS spectra of G1 and G2.

it is clear that $N(\text{H I})$ is patchy over 4–5 decades for the full range of impact parameters. These results clearly challenge the idea of a “conventional” galaxy halo encompassed by Equation 1.

In this *Letter*, we examine two very different absorber–galaxy pairs at $z \sim 0.7$ in the field of TON 153 (Q1317+274) that both clearly depart from the “conventional halo” model deduced from absorption line surveys. In § 2, we present the data. We examine the galaxy and absorption properties in § 3. In 4, we discuss these contrasting properties in the context of Λ CDM formation. Concluding remarks are given in § 5.

2. DATA AND ANALYSIS

An F702W image (PID 5984; PI Steidel) of the TON 153 field was obtained with WFPC-2 facility on board *Hubble Space Telescope* (*HST*). The image was reduced and calibrated using the WFPC-2 Associations Science Products Pipeline (WASPP⁴). The galaxy photometry was performed using the Source Extractor (SExtractor) package (Bertin & Arnouts 1996), and the K -correction was computed using the formalism of Kim, Goobar, & Perlmutter (1996). We used the GIM2D software (Simard et al. 2002) to obtain quantified morphological parameters of the galaxies.

The galaxy spectra were obtained with LRIS (Oke et al. 1995) on Keck I in 1999–March. A $1''$ wide, long slit was used with a $600 \text{ lines mm}^{-1}$ grating blazed at 7500 \AA , yielding spectral coverage from 5770 – 8340 \AA and a resolution of $\text{FWHM} \simeq 4.5 \text{ \AA}$. The LRIS spectra were reduced with IRAF⁵ using the standard NOAO *onedspec* tasks. The optical quasar spectrum was obtained with HIRES (Vogt et al. 1994) on the Keck I telescope in 1995–January. Reduction and calibration details can be found in Churchill & Vogt (2001), and Churchill, Vogt, & Charlton (2001). The UV quasar spectra were obtained with both G160L/G190H/FOS (PID 2424; PI Bahcall) and E230M/STIS (PID 8672; PI Churchill) on board *HST*. The resolving powers are $R = 170, 1300, \text{ and } 30,000$, respectively. Reduction and calibration details of the FOS spectra can be found in Churchill et al. (2000a) and of the

STIS spectrum in Ding, Charlton, & Churchill (2005). All subsequent analyses of the spectra were then performed using our own suite of graphical interactive software (following the work of Churchill et al. 1999b, 2000a; Churchill & Vogt 2001) for continuum fitting, identifying features, and measuring absorption feature properties.

3. RESULTS

In Figure 1a, we present a $40'' \times 40''$ subsection of the WFPC-2/F702W image of the TON 153 field. The galaxy G1 is centered in the image and lies at an impact parameter of $D = 58.4$ kpc from the quasar. Galaxy G2 lies at $D = 103$ kpc. In Figures 1b and c, we present $4'' \times 4''$ images of the galaxies. The LRIS spectra of G1 and G2 are presented in Figures 1d and e. A redshift of $z_{\text{G1}} = 0.6719$ was determined by Gaussian fitting to the Ca II features and $z_{\text{G2}} = 0.6610$ was determined by Gaussian fitting to the strong [O II] $\lambda 3727$ emission. G1 has a luminosity of $L_B = 4.3L_B^*$. The bulge-to-total ratio is $B/T = 0.41$. From the GIM2D modeling, the C – A morphological classification is E/S0 (see Abraham et al. 1996). G2 has $L_B = 1.8L_B^*$, $B/T = 0.81$, and a C – A morphological classification of Sab.

G2 is associated with an extensive metal-line/LLS absorber at $z = 0.6601$ (Bahcall et al. 1993, 1996; Churchill et al. 2000a; Ding, Charlton, & Churchill 2005), with $W_r(\text{Ly}\alpha) = 1.48$, $W_r(\text{Ly}\beta) = 0.84$, $W_r(2796) = 0.34$, $W_r(1548) = 0.32$, and $W_r(1031) \leq 0.13 \text{ \AA}$ (3σ). The rotation curve of G2 was presented by Steidel et al. (2002), who showed that the bulk of the Mg II absorbing gas kinematics are offset by 180 km s^{-1} from the G2 systemic velocity in the direction of galaxy rotation. The CIV absorption spans the same velocity range as Mg II, though the strongest component likely arises in a separate phase at the G2 systemic velocity (Churchill & Steidel 2003; Ding, Charlton, & Churchill 2005). As shown in Figure 2a, there is a remarkable complex of five Ly α absorbers spanning the redshift of G1 in the G190H FOS spectrum, first reported by Bahcall et al. (1996). Gaussian deblending confirms five statistically significant Ly α components with redshifts (rest-frame equivalent widths [\AA]) $z = 0.66914$ (0.65 ± 0.05), 0.67157 (0.39 ± 0.05), 0.67355 (0.78 ± 0.16), 0.67559 (0.79 ± 0.20), and 0.67707 (0.26 ± 0.08). The total equivalent width of the complex is $W_r(\text{Ly}\alpha) = 2.87 \text{ \AA}$. The offset tick is the redshift of G1⁶.

⁴ Developed by the Canadian Astronomy Data Centre (CADC) and the Space Telescope–European Coordinating Facility (ST-ECF): <http://archive.stsci.edu/hst/wfpc2/pipeline.html>

⁵ IRAF is written and supported by the IRAF programming group at the National Optical Astronomy Observatories (NOAO) in Tucson, Arizona. NOAO is operated by the Association of Universities for Research in Astronomy (AURA), Inc. under cooperative agreement with the National Science Foundation.

⁶ We note that Chen et al. (2001b) assign the $z = 0.6716$ cloud to G1; how-

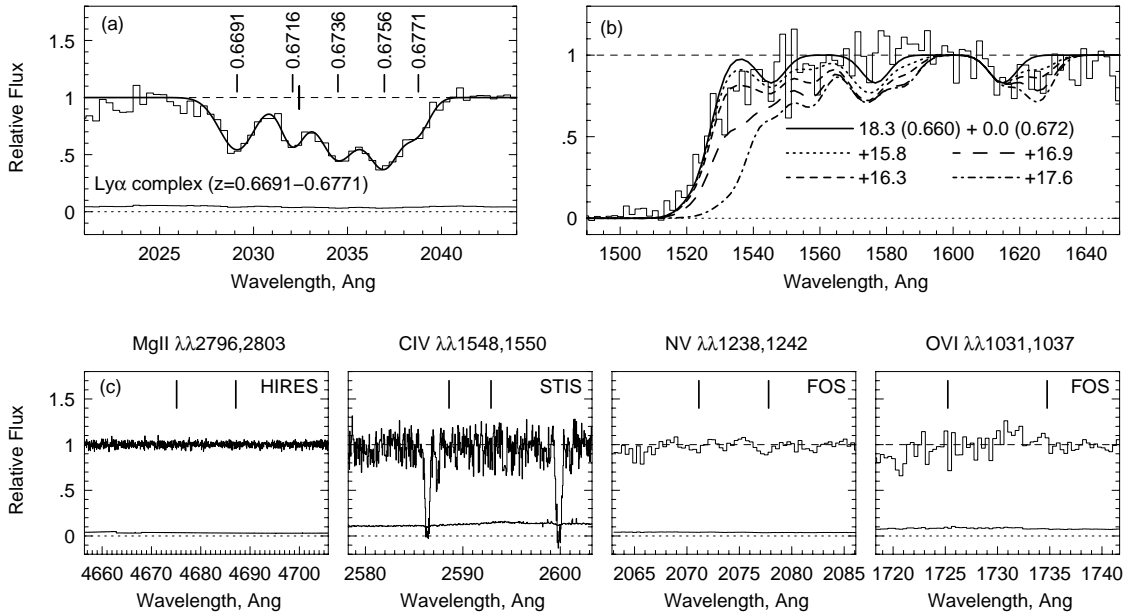


FIG. 2.— (a) The Ly α complex (FOS/G190H) spanning $0.6691 \leq z \leq 0.6771$. The lowered tick corresponds to $z_{G1} = 0.6719$. — (b) The Lyman limit region (FOS/G160L), illustrating our modeling (see text) of the break for the Ly α complex in panel (c). — (c) Regions of anticipated MgII (HIRES), CIV (STIS/E230M), and NV and OVI (FOS/G190H) doublet absorption at the redshift of G1, covering ± 1200 km s $^{-1}$ (rest-frame) with respect to $z = 0.6719$, or $0.6652 \leq z \leq 0.6785$. The ticks provide the expected locations for the doublets. The STIS feature are Galactic FeII absorption.

In Figure 2b, we show the G160L FOS spectrum of the Lyman limit for the Ly α complex encompassing G1 and G2. Bahcall et al. (1993) measured $\tau_{LL} \geq 3.5$, whereas Churchill et al. (2000a) obtained $\tau_{LL} \geq 5.4$. From this we infer $\log N(\text{HI}) \geq 17.9$ [cm $^{-2}$]. However, simultaneous fitting to the Ly α , Ly β , and LL absorption at $z = 0.6601$ yields $\log N(\text{HI}) \simeq 18.3 \pm 0.3$. We show this fit as the solid curve in Figure 2b. We then modeled the Lyman limit for the G1 Ly α complex to constrain the total $N(\text{HI})$. We tested cases that both included and excluded the LL break absorption from the $z = 0.6601$ system with various continuum extrapolations below the LL break. Applying the curve of growth to the Ly α equivalent widths, we assigned equal Doppler b parameters to all five components and varied these b parameters [$N(\text{HI})$ is dominated by the $z = 0.6736$ and 0.6756 clouds]. We show four selected models ($b = 30, 35, 40,$ and 45 km s $^{-1}$) as the short-dash-dot [total G1 complex $\log N(\text{HI}) = 17.8$], long-dash [16.9], short-dash [16.3], and dot-dot [15.8] curves, respectively. Using the χ^2 statistic, we find that G1 Ly α complex has $\tau_{LL} \leq 0.39$ (3σ) and estimate that no *single* component can have $\log N(\text{HI})$ exceeding ~ 16.5 .

In Figure 2c, the expected regions for MgII, CIV, NV, and OVI metal-line absorption are shown. Ticks provide the predicted locations of the doublet members at $z_{G1} = 0.6719$. The regions cover ± 1200 km s $^{-1}$ (rest-frame) relative to G1 over which *both* doublet members could be detected ($0.6652 \leq z \leq 0.6785$, spanning the G1 Ly α complex). We obtained 3σ rest-frame equivalent width limits of 7 mÅ, 0.03 Å, 0.11 Å, and 0.21 Å for MgII, CIV, NV, and OVI, respectively. For MgII and CIV, $\log N(\text{MgII}) \leq 11.1$ and $\log N(\text{CIV}) \leq 12.9$, independent of broadening. Assuming $T = 3 \times 10^5$ K, where the OVI fraction peaks in collisionally ionized gas, we find $\log N(\text{NV}) \leq 13.8$ and $\log N(\text{OVI}) \leq 15.0$.

4. DISCUSSION

ever, the equivalent widths they report appear to be misquoted within this Ly α complex.

4.1. On the Covering Factor

Applying the R^* and β parameters quoted in § 1 to Equation 1, we obtain “halo” boundaries for G1 of $R(L) = 73$ kpc for $W_r(2796) \geq 0.3$ Å and $\tau_{LL} \geq 1$. For $W_r(2796) \geq 0.02$ Å, we obtain $R(L) = 123$ kpc, and for $W_r(1548) \geq 0.17$ Å, $R(L) = 350$ kpc. In Figure 1a, we illustrate the $R(L)$ boundaries for the LLS and MgII thresholds. The solid circle represents $W_r(2796) \geq 0.3$ Å and $\tau_{LL} \geq 1$, and the dash-dash circle represents $W_r(2796) \geq 0.02$ Å. The $R(L)$ boundary for CIV extends beyond the image section. For G2, we obtain $R(L) = 62$ kpc for $W_r(2796) \geq 0.3$ Å and $\tau_{LL} \geq 1$, and $R(L) = 228$ kpc for $W_r(1548) \geq 0.17$ Å.

For G1 MgII absorption, the 3σ equivalent width upper limit is a factor of $\simeq 40$ below 0.3 Å (the minimum expected value) at the location $D/R(L) = 0.79$. For weak MgII absorption, the limit is $\simeq 3$ times below the 0.02 Å sensitivity threshold at $D/R(L) = 0.47$. The limit for CIV is a factor of $\simeq 6$ below the 0.17 Å sensitivity threshold at $D/R(L) = 0.16$. Ly α absorption with $W_r(\text{Ly}\alpha) \geq 0.30$ Å is expected within $D \leq 530$ kpc (Chen et al. 1998, 2001b) and the five-component G1 Ly α complex has total $W_r(\text{Ly}\alpha) = 2.87$ Å. However, at $D = 58$ kpc, the expectation is that LLS absorption would be detected in the “halo” of G1 and no clear feature is present to a level suggesting $\tau_{LL} \leq 0.4$. For G2, the conditions are quite different. MgII and LLS absorption arises at $D/R(L) = 1.66$, well beyond the “halo” boundary, whereas the CIV absorption arises at $D/R(L) = 0.45$, per expectations.

There is now mounting evidence (this work; Bechtold & Ellingson 1992; Churchill, Kacprzak, & Steidel 2005; Tripp & Bowen 2005) that $C_f f_{gal} \mathcal{K} < 1$ for MgII absorption. The very nature of selecting absorber-galaxy pairs may have strongly contributed to previous inferences that $C_f f_{gal} \mathcal{K} = 1$ and the applicability of Equation 1. Results for the G1 and G2 galaxies suggest that, in some cases, this is true for CIV and LLS absorption as well. A full

assessment of the possible selection bias is highly needed (e.g., Charlton & Churchill 1996). The application of a non-standardized model of galaxy halos should now be incorporated into our appreciation of galaxy halos in the context of Λ CDM formation models.

4.2. Comparing the G1 and G2 Gas Properties

In addition to the lack of metal-lines, the $\Delta v \simeq 1420 \text{ km s}^{-1}$ velocity spread of the G1 Ly α complex at $D = 58 \text{ kpc}$ is difficult to understand as a “conventional” gas halo. On the other hand, the G2 associated absorption at $D = 103 \text{ kpc}$ has $\Delta v \simeq 200 \text{ km s}^{-1}$ and is consistent with a photoionized halo, including an optically thick phase ($T \simeq 8000 \text{ K}$) and a diffuse optically thin phase ($T \simeq 20,000 \text{ K}$) (see Figure 6 and Table 9 of Ding, Charlton, & Churchill 2005). Accounting for $\log N(\text{H I}) = 18.3$ adopted in this work, the cloud metallicities from Ding, Charlton, & Churchill (2005) could be as high as $\log(Z/Z_{\odot}) = -0.4$.

Adopting the solar abundance pattern of Holweger (2001), we examined Cloudy (Ferland 2001) photoionization and collisional (Sutherland & Dopita 1993) models of the G1 Ly α complex in order to constrain the metallicities. For photoionization, the lack of [O II] emission (star formation) in G1 motivates an ultraviolet background only model at $z = 0.7$ (Haardt & Madau 1996). Using the $N(\text{Mg II})$ and $N(\text{C IV})$ limits, we computed a grid of $Z_{\text{max}} \equiv \log Z/Z_{\odot}$, the upper limit on metallicity, for each Ly α cloud as a function of ionization parameter in steps of $\Delta \log U = 0.2$ over the range $-3.5 \leq \log U \leq -0.5$ and $N(\text{H I}) \leq 16.5$, determined from the Ly α curve of growth in steps of $\Delta b = 5 \text{ km s}^{-1}$.

For Mg II, $Z_{\text{max}} \simeq \text{constant}$ for $\log U \leq -2.5$ for a given $N(\text{H I})$, and we find $Z_{\text{max}} \simeq \log[14.4/N(\text{H I})]$. At $-1.0 \leq \log U \leq -0.5$, where C IV peaks, $Z_{\text{max}} \simeq \log[12.5/N(\text{H I})]$. Assuming $b_{\text{H}} \simeq 40 \text{ km s}^{-1}$ (Williger et al. 2006), for the three lowest $W_r(\text{Ly } \alpha)$ clouds ($z = 0.6771, 0.6716, \text{ and } 0.6691$), the most stringent limits are $Z_{\text{max}} \simeq -1.2, -1.6, \text{ and } -2.6$ from C IV; Z_{max} is less constrained with decreasing U for $\log U \leq -1.0$ such that the $z = 0.6771$ and 0.6716 clouds can be consistent with solar metallicity. However, for the $z = 0.6691$ cloud, Mg II yields a hard limit of $Z_{\text{max}} \simeq -0.8$. Assuming $b_{\text{H}} = 20 \text{ km s}^{-1}$ the three clouds have hard upper limits of $Z_{\text{max}} \simeq -0.5, -1.5, \text{ and } -1.8$ from Mg II for $\log U \leq -2.5$. An α -group enhancement would decrease these hard limits on Z_{max} by as much as 0.3–0.5 dex. The most severe constraints are $Z_{\text{max}} \simeq -1.6, -3.0, \text{ and } -3.2$, respectively, from C IV for $-1.0 \leq \log U \leq 0.5$.

For the collisional ionization models, we computed⁷ $Z_{\text{max}}(X)$ for each Ly α cloud as a function temperature (in steps of $\Delta \log T = 0.05 \text{ K}$) using the ionization fractions, $f(X)$, for H I, C IV, and O VI. The $N(\text{C IV})$ and $N(\text{O VI})$ limits and $N(\text{H I})$ are constrained by the curve of growth as a function of temperature, assuming b_x is thermal. The O VI limit dominates for $T \geq 2 \times 10^5 \text{ K}$ [$b_{\text{H}} \geq 57 \text{ km s}^{-1}$], and the C IV limit dominates for lower T [$b_{\text{H}} \leq 57 \text{ km s}^{-1}$]. At this transition T , the hard limit is $Z_{\text{max}} = -0.6$ for the $z = 0.6691$ cloud, and the hard limit is $Z_{\text{max}} = -1.0$ for the two largest $W_r(\text{Ly } \alpha)$ clouds ($z = 0.6736$ and 0.6756). For the latter two clouds, if $T = 3 \times 10^5 \text{ K}$, where O VI peaks, then $\log N(\text{H I}) \simeq 14.7$ and $Z_{\text{max}} \simeq -2.8$; at $T = 10^5 \text{ K}$, where C IV peaks, $\log N(\text{H I}) \simeq 16.0$ and $Z_{\text{max}} \simeq -3.0$.

We consider the Λ CDM models of Davé et al. (1999) at $z \sim 1$ as a guide to expectations for the gas properties in the

proximity of G1 and G2. At $D \simeq 60 \text{ kpc}$ (G1), the matter overdensities range from $10 \leq \Delta\rho/\rho \leq 100$, where $\sim 80\%$ of the absorbers arise in shocked gas (accreting onto filaments or galaxy halos) and $\sim 20\%$ of absorbers arise in a photoionized, adiabatically cooling, diffuse phase. For $D \simeq 100 \text{ kpc}$ (G2), overdensities range from a few $\leq \Delta\rho/\rho \leq 30$, where $\sim 60\%$ arise in the shocked phase and $\sim 40\%$ arise in the diffuse phase.

If the dominant clouds in the G1 Ly α complex are collisionally ionized, the inferred properties are $T \sim 10^{5.0-5.5} \text{ K}$, $-1.0 \leq Z_{\text{max}} \leq -3.0$, $14.5 \leq \log N(\text{H I}) \leq 15.5$, and $\Delta\rho/\rho \simeq 100$. In Λ CDM cosmology, at $z \simeq 3$ this gas would have been in the photoionized diffuse phase with $\Delta\rho/\rho \sim 10$ (Davé et al. 1999; Schaye 2001). The mean metallicity of photoionized, diffuse Ly α forest clouds at $z \simeq 3$ is $[\text{C/H}] \simeq -2.5$ (Cowie & Songaila 1998), an enrichment level consistent with the inferred Z_{max} for collisional ionization in the dominant clouds in the G1 Ly α complex at $z = 0.7$. A possible scenario is that the dominant G1 clouds could have been enriched to $[\text{C/H}] \simeq -2.5$ by $z = 3$ while in the diffuse phase and transitioned to shock heated gas by $z = 0.7$, presumably due to their accreting onto a filamentary structure in the vicinity of G1, without having been further enriched by G1. It is less likely that the dominant clouds remained in the diffuse phase from $z = 3$ to $z = 0.7$ for which the Davé et al. (1999) and Schaye (2001) models predict $\Delta\rho/\rho \leq 10$, $\log N(\text{H I}) \simeq 14$, and $T \simeq 10^{4-4.3} \text{ K}$. The dominant clouds cannot have this low $N(\text{H I})$ even for $b_{\text{H}} > 100 \text{ km s}^{-1}$, and even the weakest clouds would have to be highly turbulent ($b_{\text{H}} > 80 \text{ km s}^{-1}$). Songaila & Cowie (1996) reported that clustered Ly α lines at $z = 3$ are structured such that higher ionization clouds reside at the velocity extremes and suggest that this is due to a layered structure to the gas and is related to the physics of collapse. A high resolution spectrum of the Lyman series of the G1 Ly α complex could be very informative regarding the physics underlying the gas.

The conditions of the G2 absorption is consistent with a diffuse phase (Ding, Charlton, & Churchill 2005). A $\log N(\text{H I}) = 18.3$ corresponds to $\Delta\rho/\rho > 1000$ at $z \leq 1$, that would have arisen from an overdensity of 100 at $z = 3$ (Davé et al. 1999; Schaye 2001). This implies the gas was already in the shocked phase by $z = 3$. It is possible that the gas associated with the formation of G2 evolved more rapidly than that of G1 and virialized by $z \simeq 3$. If so, there would be time for additional metallicity enrichment in this highly evolved structure and for reprocessing from G2 to re-establish a diffuse phase following the post-shock condensed phase. The strong O II emission in G2 suggests star formation may have played a role, perhaps inducing localized fountains and outflows. This scenario is analogous to the wind-driven gas observed in $z = 3$ galaxies reported by Adelberger et al. (2005) and Simcoe et al. (2006).

5. CONCLUDING REMARKS

Even if the G1 and G2 gas structures extend $\simeq 3000 \text{ km s}^{-1}$ between the galaxies (see, Bahcall et al. 1996), inhomogeneities in the overdensities on Mpc scales do not rule out the possible very different evolution of the gas associated with the two galaxies, as outlined above. The presence of weak Ly α lines in the range $0.660 \leq z \leq 0.672$ would be highly suggestive of an H I bridge connecting the galaxies G1 and G2. Both these two very dissimilar absorber–galaxy pairs exhibit properties inconsistent with the conventional model of galaxy halos (i.e., $C_f f_{\text{gal}} \mathcal{K} = 1$ and Equation 1) deduced from quasar

⁷ $Z_{\text{max}}(X) = \log[N_{\text{lim}}(X)/N(\text{H I})] + \log[f(\text{H I})/f(X)] - \log(X/\text{H})_{\odot}$.

absorption line surveys. Selection methods may have played an important role (see Charlton & Churchill 1996); the notion that galaxy “halos” exhibit a level of homogeneity in which they can be characterized by a standardized covering factor, geometry, and boundary should be viewed critically. We have suggested that the heterogeneous nature of extended gas surrounding galaxies at impact parameters of several 10s to a 100 kiloparsecs may be strongly related to the range of overdensities from which the galaxy and the gaseous environment evolved in the context of Λ CDM models.

Support for this research through grant HST-AR-10644.01-

A was provided by NASA via the Space Telescope Science Institute, which is operated by the Association of Universities for Research in Astronomy, Inc., under NASA contract NAS 5-26555. G.G.K acknowledges support from Sigma-Xi Grants in Aid of Research. J.L.E. acknowledges support from Research Cluster Fellowship from NMSU and a Graduate Student Fellowship from NASA’s New Mexico Space Grant Consortium.

Facilities: HST (WFPC–2, STIS, FOS), Keck I (HIRES, LRIS).

REFERENCES

- Abraham, R. G., van den Bergh, S., Glazebrook, K., Ellis, R. S., Santiago, B. X., Surma, P., & Griffiths, R. E. 1996, *ApJS*, 107, 1
- Adelberger, K. L., Shapley, A. E., Steidel, C. C., Pettini, M., Erb, D. K., & Reddy, N. A. 2005, *ApJ*, 629, 636
- Bahcall, J. N., et al. 1993, *ApJS*, 87, 1
- Bahcall, J. N., et al. 1996, *ApJ*, 457, 19
- Bechtold, J., & Ellingson, E. 1992, *ApJ*, 396, 20
- Bergeron, J., & Boissé, P. 1991, *A&A*, 243, 334
- Bertin, E., & Arnouts, S. 1996, *A&AS*, 117, 393
- Charlton, J. C., & Churchill, C. W. 1996, *ApJ*, 465, 631
- Chen, H.-W., Lanzetta, K. M., Webb, J. K., & Barcons, X. 1998, *ApJ*, 498, 77
- Chen, H.-W., Lanzetta, K. M., & Webb, J. K. 2001a, *ApJ*, 556, 158
- Chen, H.-W., Lanzetta, K. M., Webb, J. K., & Barcons, X. 2001b, *ApJ*, 559, 654
- Churchill, C. W., Kacprzak, G. G., & Steidel, C. C. 2005, in *Probing Galaxies through Quasar Absorption Lines*, IAU 199 Proceedings, eds. P. R. Williams, C.-G. Shu, & B. Ménard (Cambridge: Cambridge University Press), p. 24
- Churchill, C. W., Mellon, R. R., Charlton, J. C., Jannuzi, B. T., Kirhakos, S., Steidel, C. C., & Schneider, D. P. 2000a, *ApJS*, 130, 91
- Churchill, C. W., Rigby, J. R., Charlton, J. C., & Vogt, S. S. 1999b, *ApJS*, 120, 51
- Churchill, C., & Steidel, C. 2003, *ASSL Vol. 281: The IGM/Galaxy Connection. The Distribution of Baryons at $z = 0$* , 149
- Churchill, C. W., & Vogt, S. S. 2001, *AJ*, 122, 679
- Churchill, C. W., Vogt, S. S., & Charlton, J. C. 2003, *AJ*, 125, 98
- Cowie, L. L., & Songaila, A. 1998, *Nature*, 394, 44
- Davé, R., Hernquist, L., Katz, N., & Weinberg, D. H. 1999, *ApJ*, 511, 521
- Davé, R., et al. 2001, *ApJ*, 552, 473
- Davé, R., Hellsten, U., Hernquist, L., Katz, N., & Weinberg, D. H. 1998, *ApJ*, 509, 661
- Ding, J., Charlton, J. C., & Churchill, C. W. 2005, *ApJ*, 621, 615
- Ferland, G. 2001, *Hazy, A Brief Introduction to Cloudy 96.00*
- Haardt, F., & Madau, P. 1996, *ApJ*, 461, 20
- Holmberg, E. 1975, in *Stars and Stellar Systems: Galaxies and the Universe*, eds. A. Sandage & J. Kristian, Vol. 9, p. 123
- Holweber, H. 2001, *AIP Conf. Proc. 598: Joint SOHO/ACE workshop “Solar and Galactic Composition”*, 598, 23
- Kim, A., Goobar, A., & Perlmutter, S. 1996, *PASP*, 108, 190
- Lanzetta, K. M., Bowen, D. V., Tytler, D., & Webb, J. K. 1995, *ApJ*, 442, 538
- Le Brun, V., Bergeron, J., Boisse, P., & Christian, C. 1993, *A&A*, 279, 33
- Mo, H. J., & Mao, S. 2002, *MNRAS*, 333, 768
- Mo, H. J., Mao, S., & White, S. D. M. 1998, *MNRAS*, 295, 319
- Oke, J. B., et al. 1995, *PASP*, 107, 375
- Schaye, J. 2001, *ApJ*, 559, 507
- Sembach, K. R., Tripp, T. M., Savage, B. D., & Richter, P. 2004, *ApJS*, 155, 351
- Simard, L., Willmer, C. N. A., Vogt, N. P., Sarajedini, V. L., Philips, A. C., Weiner, B. J., Koo, D. C., Im, M., Illingworth, G. D., & Faber, S. M. 2002, *ApJS*, 142, 1
- Simcoe, R. A., Sargent, W. L. W., Rauch, M., & Becker, G. 2006, *ApJ*, 637, 648
- Songaila, A., & Cowie, L. L. 1996, *AJ*, 112, 335
- Steidel, C. C. 1995, in *QSO Absorption Lines*, ed. G. Meylan, (Springer-verlag: Berlin Heidelberg), p. 139
- Steidel, C. C., Dickinson, M., Meyer, D. M., Adelberger, K. L., & Sembach, K. R. 1997, *ApJ*, 480, 586
- Steidel, C. C., Dickinson, M., & Persson, S. E. *ApJ*, 437, L75 (SDP94)
- Steidel, C. C., Kollmeier, J. A., Shapely, A. E., Churchill, C. W., Dickinson, M., & Pettini, M. 2002, *ApJ*, 570, 526
- Stengler-Larrea, E. A., et al. 1995, *ApJ*, 444, 64
- Sutherland, R. S., & Dopita, M. A. 1993, *ApJS*, 88, 253
- Tripp, T. M., Aracil, B., Bowen, D. V., & Jenkins, E. B. 2006, *ApJ*, 643, L77
- Tripp, T. M., & Bowen, D. V. 2005, in *Probing Galaxies through Quasar Absorption Lines*, IAU 199 Proceedings, eds. P. R. Williams, C.-G. Shu, & B. Ménard (Cambridge: Cambridge University Press), p. 5
- Tumlinson, J., Shull, J. M., Giroux, M. L., & Stocke, J. T. 2005, *ApJ*, 620, 95
- Vogt, S. S., et al. 1994, *SPIE*, 2198, 362
- Williger, G. M., Heap, S. R., Weymann, R. J., Davé, R., Ellingson, E., Carswell, R. F., Tripp, T. M., & Jenkins, E. B. 2006, *ApJ*, 636, 631
- White, S. D. M., & Rees, M. J. 1978, *MNRAS*, 183, 341